HHS Public Access

Author manuscript

Nat Med. Author manuscript; available in PMC 2015 April 24.

Published in final edited form as:

Nat Med. 2014 November ; 20(11): 1310–1314. doi:10.1038/nm.3737.

An *in vivo* model of human small intestine using pluripotent stem cells

Carey L Watson[1,2,10], **Maxime M Mahe**[1,10], **Jorge Múnera**[3], **Jonathan C Howell**[4], **Nambirajan Sundaram**[1], **Holly M Poling**[1], **Jamie I Schweitzer**[3], **Jefferson E Vallance**[5], **Christopher N Mayhew**[3], **Ying Sun**[6], **Gregory Grabowski**[6,7], **Stacy R Finkbeiner**[8], **Jason R Spence**[8], **Noah F Shroyer**[5,9], **James M Wells**[3], and **Michael A Helmrath**[1,2]

[1]Department of Pediatric General and Thoracic Surgery, Cincinnati Children's Hospital Medical Center, Cincinnati, Ohio, USA

[2]Department of General Surgery, University of Cincinnati, Cincinnati, Ohio, USA

[3]Department of Developmental Biology, Cincinnati Children's Hospital Medical Center, Cincinnati, Ohio, USA

[4]Department of Endocrinology, Cincinnati Children's Hospital Medical Center, Cincinnati, Ohio, USA

[5]Department of Gastroenterology, Hepatology and Nutrition, Cincinnati Children's Hospital Medical Center, Cincinnati, Ohio, USA

[6]Department of Human Genetics, Cincinnati Children's Hospital Medical Center, Cincinnati, Ohio, USA

[7]Synageva Corporation, Lexington, Massachusetts, USA

[8]Department of Internal Medicine, University of Michigan, Biomedical Science Research Building, Ann Arbor, Michigan, USA

[9]Department of Medicine, Section of Gastroenterology & Hepatology, Baylor College of Medicine, Houston, Texas, USA

Abstract

Differentiation of human pluripotent stem cells (hPSCs) into organ-specific subtypes offers an exciting avenue for the study of embryonic development and disease processes, for pharmacologic

Correspondence should be addressed to M.A.H. (michael.helmrath@cchmc.org).

[10]These authors contributed equally to this work.

AUTHOR CONTRIBUTIONS

C.L.W. and M.M.M. designed the experiments, performed the surgeries, collected and assembled data and wrote the manuscript. J.M., J.C.H., N.S., H.M.P., J.I.S., J.E.V., C.N.M., Y.S., G.G., S.R.F. and J.R.S. collected and provided study materials. N.F.S. and J.M.W. were involved in the study design and wrote and approved the manuscript. M.A.H. designed the study, wrote the manuscript and finally approved the manuscript. All authors discussed the results and commented on the manuscript.

COMPETING FINANCIAL INTERESTS

The authors declare no competing financial interests.

Note: Any Supplementary Information and Source Data files are available in the online version of the paper.

studies and as a potential resource for therapeutic transplant[1,2]. To date, limited *in vivo* models exist for human intestine, all of which are dependent upon primary epithelial cultures or digested tissue from surgical biopsies that include mesenchymal cells transplanted on biodegradable scaffolds[3,4]. Here, we generated human intestinal organoids (HIOs) produced *in vitro* from human embryonic stem cells (ESCs) or induced pluripotent stem cells (iPSCs)[5,6] that can engraft *in vivo*. These HIOs form mature human intestinal epithelium with intestinal stem cells contributing to the cryptvillus architecture and a laminated human mesenchyme, both supported by mouse vasculature ingrowth. *In vivo* transplantation resulted in marked expansion and maturation of the epithelium and mesenchyme, as demonstrated by differentiated intestinal cell lineages (enterocytes, goblet cells, Paneth cells, tuft cells and enteroendocrine cells), presence of functional brush-border enzymes (lactase, sucrase-isomaltase and dipeptidyl peptidase 4) and visible subepithelial and smooth muscle layers when compared with HIOs *in vitro.* Transplanted intestinal tissues demonstrated digestive functions as shown by permeability and peptide uptake studies. Furthermore, transplanted HIO-derived tissue was responsive to systemic signals from the host mouse following ileocecal resection, suggesting a role for circulating factors in the intestinal adaptive response[7–9]. This model of the human small intestine may pave the way for studies of intestinal physiology, disease and translational studies.

Because of the complexity of a vascularized hollow organ such as the intestine, the development of an adequate human model for its study and replacement following surgery or pathological processes has proven to be a seemingly impossible task. Methods for studying the human intestine have largely required *in vitro* culture systems or have relied on animal models to address numerous translational questions, and these do not always translate well in human studies. Traditional intestinal epithelial primary culture techniques were mostly limited to tissue culture technologies, such as organ cultures or intestinal cell lines that do not recapitulate the hierarchy of stem cells to differentiated cells[10]. The recent identification of intestinal stem cells and conditions appropriate for human epithelial culture has overcome many of these obstacles[11,12]. Successful *in vivo* engraftment of epithelial cultures, however, remains challenging because of the need for a supporting mesenchyme[13–17], as exists in models exposing host mesenchyme following mucosal injury[18,19].

In contrast to using primary cell culture approaches that require surgical samples, we recently described an *in vitro* approach for generating HIOs *de novo* from hPSCs[5]. This technique allows for the robust development of human intestinal tissue, including epithelium with a surrounding and supportive mesenchyme, for *in vitro* studies. Although HIOs have some intestinal functionality *in vitro*, this model is insufficient for investigating the impact of broad physiological stimuli on human intestinal tissues. For this reason, we developed an *in vivo* HIO engraftment model and used it to generate mature, functional human intestinal tissues *in vivo* that respond to the physiological stimuli triggered by ileocecal resection.

To establish an *in vivo* HIO model, we generated HIOs from human ESCs or iPSCs as previously described[5,6]. The differentiation process took approximately 35 d (Fig. 1a and Supplementary Fig. 1a) and produced HIOs with columnar intestinal epithelium surrounded by a supporting mesenchyme (Fig. 1b and Supplementary Fig. 1b). We then embedded the

HIOs into type I collagen and transplanted them under the kidney capsule of immunocompromised nonobese diabetic severe combined immunodeficiency interleukin-2Rγ^{null} (NSG) mice and allowed them to mature and grow for 6 weeks (Fig. 1a and Supplementary Fig. 1d,*e*). At the time of harvest, the HIOs had grown considerably in size, upwards of 50- to 100-fold larger in volume (Fig. 1c,d and Supplementary Figs. 1c and 2a) and were highly vascularized (Fig. 1c). Of note, 92.4% of the transplanted HIOs successfully engrafted under the kidney capsule (Supplementary Fig. 1f). Visual inspection of tissues revealed intestinal morphology (Fig. 1d) with mucous-filled lumens and well-developed sheets of villi, each with its own central capillary network (Fig. 1e). Histologically, this engrafted tissue resembled native human intestine with crypt-villus architecture and underlying laminated submucosal layers including lamina propria, muscularis mucosa and submucosa and outer smooth muscle layers (Fig. 2a and Supplementary Fig. 2c). When compared with their *in vitro* counterparts (data not shown)[5], the engrafted tissue *in vivo* appeared more mature and differentiated, with all major intestinal cell lineages, including enterocytes, goblet cells, Paneth cells, enteroendocrine cells and tuft cells, located within appropriate regions of the crypt-villus axis (Fig. 2b–d and Supplementary Fig. 2d–g). Paneth cells were located within crypt bases as expected rather than scattered throughout the epithelium (Fig. 2b,c)[12]. Transmission electron microscropy (TEM) revealed a brush border with well-developed tight junctions similar to that of HIOs *in vitro* (Supplementary Fig. 3a); however, mature goblet cells and enteroendocrine cells, as seen within the epithelium of engraftments (Supplementary Fig. 3b,c), were not present in TEM of HIOs *in vitro* (data not shown). Within the epithelium, we observed increased relative expression of genes characteristic of the epithelial cell types when comparing engraftments to HIOs *in vitro* (Supplementary Fig. 4a–g). We found that blood vessels within the engraftment stained positive for mouse-specific panendothelial cell antigen (mMECA-32) (Fig. 2e). The engrafted tissue was also actively proliferating within discreet crypts, as revealed by incorporation of 5-ethynyl-2′-deoxyuridine (Edu) (Fig. 2f). Using transgenic human LGR5 reporter HIOs to trace intestinal stem cells, we found that actively proliferating labeled stem cells were present within the HIOs and localized to the base of the crypts in the engraftment (Supplementary Fig. 5a–d). Additionally, the engrafted tissue expressed the stem cell marker ASCL2 (Supplementary Fig. 5e,f), and we were able to generate enteroids derived from the epithelium of engraftments, further demonstrating the existence of an intestinal stem cell pool (Supplementary Fig. 5g–k). These data suggest that HIOs undergo considerable maturation into mature intestinal tissue following engraftment *in vivo*.

Cross-talk between the adjacent mesenchyme and intestinal epithelium is known to play a major role during GI development[20]. It was previously shown that the supporting mesenchyme develops alongside the intestinal epithelium of HIOs *in vitro*[5] and contains immature populations of subepithelial myofibroblasts, fibroblasts and smooth muscle cells[21,22]. We investigated whether HIO mesenchyme also developed into more mature, differentiated cell types following engraftment *in vivo*. The non-epithelial regions of the engrafted tissue stained positive for the mesenchymal marker vimentin (VIM) and included several laminated subepithelial layers, including distinct smooth muscle layers positive for α–smooth muscle actin (α-SMA), revealing the mesenchymal contribution of the

engraftment (Fig. 2g). Additionally, dual staining for α-SMA and VIM revealed a pericryptal sheath (Fig. 2g) of intestinal subepithelial myofibroblasts (ISEMFs) which are known to support *in vitro* and *in vivo* growth of human small intestinal epithelial stem cells[3,21,23]. Likewise, the intestinal epithelium has been shown to contribute appropriate signals for the development of the subepithelial mesenchymal layers including lamina propria, ISEMFs and muscularis mucosa[20] leading to appropriate laminations of the subepithelium (Fig. 2a,g). In addition to the maturity of smooth muscle layers histologically, relative expression of desmin and α-SMA was increased in HIOs engrafted *in vivo* as compared to HIOs *in vitro* (Supplementary Fig. 4h,i). TEM of the engraftments revealed smooth muscle cells with parallel orientation similar to that of adult intestine (Supplementary Fig. 3d). These data are consistent with published reports that successful engraftment and maturation of human intestinal tissues requires the presence of a mesenchymal niche[13–16,19]. For example, lack of a mesenchymal component has resulted in failure of engraftment[3,14,15], whereas including mesenchymal cells along with epithelium resulted in successful engraftment[3,4,14–17].

As our engraftments contained a variety of mesenchymal cell types, including endothelial cells, we next investigated which components were of human origin and which were from the host. As expected, HIO epithelium was completely of human origin and stained positive for a human nuclear antigen (HuNuc) (Fig. 2h). In addition, the majority of tissue of mesenchymal origin, including lamina propria, muscularis mucosa, submucosa and smooth muscle layers, also stained positive for HuNuc (Fig. 2i). In contrast, the majority of blood vessels were of mouse origin as they stained positive for mMECA-32 (Fig. 2e). The blood supply of the engrafted HIO was supported by mouse vasculature, as demonstrated by positive labeling of endothelium with FITC-conjugated tomato lectin tail vein injection (Supplementary Fig. 6a–d). Few blood vessels of human origin were positive for human-specific panendothelial cell antigen in the engraftment, and these were not connected to the mouse vasculature (Supplementary Fig. 6e,f). Lymphatic vessels were of mouse origin and stained positive for mouse-specific lymphatic vessel endothelial hyaluronan receptor 1 (LYVE-1) (Supplementary Fig. 6g).

Engraftment of PSC-derived pancreatic progenitor cells has been shown to enhance development of islet cells *in vivo*[24]. We analyzed the impact of *in vivo* growth on the maturity of our engraftments at 6 weeks as compared to HIOs *in vitro* at a similar time point (35 d plus 6 weeks *in vitro*) by determining the expression of several markers of mature epithelium at both the mRNA and protein levels. We observed marked increases in mRNA and/or protein expression of markers characteristic of differentiated enterocytes, including dipeptidyl peptidase 4 (DPPIV), glucose transporter type 2 (GLUT2), sucrose-isomaltase (SIM) and villin (VIL), compared to HIOs *in vitro* (Fig. 3a,b,e,f,i and Supplementary Fig. 4b,*g*)[25]. Additionally, we also looked at the brush border enzymes alkaline phosphatase (ALPI) and lactase (LCT), as well as markers of secretory cell types, including enteroendocrine (gastric inhibitory peptide (GIP) and chromogranin A (CHGA)), goblet (mucin 2 (MUC2)) and Paneth cells (lysozyme (LYSO)). For each of these markers, there were also marked increases in mRNA and protein expression in engrafted HIOs (Fig.

3c,d,g–i and Supplementary Fig. 4c–f). Therefore, we concluded that *in vivo* growth promotes maturation of the intestinal tissue.

Given the mature phenotype of engrafted HIOs *in vivo*, we postulated that these tissues might represent a new model to study *in vivo* physiology of the human gut. We therefore investigated whether engrafted HIOs could respond to physiologic cues elicited by intestinal resection. Humoral factors have been suggested to be involved in the intestinal adaptive response. In rats connected in a parabiotic relationship via vascular anastomosis, surgical resection in one rat led to increased intestinal proliferation in the parabiotic partner[7]. However, there is no model available to investigate this phenomenon with human intestine. Here, we used a model of ileocecal resection (ICR)[26] in the transplanted mice to investigate whether circulating humoral factors that are stimulated in response to intestinal resection could affect engrafted human intestinal tissues in the kidney. We randomized mice with HIO engraftments at our 6-week time point following transplant to sham (transection and reanastomosis) or ICR groups and quantified morphometric factors associated with intestinal adaptation including crypt depth, villus height, epithelial proliferation, crypt fission and thickness of the circular and longitudinal smooth muscle layers (tunica muscularis) (Fig. 4a). Adaptation in NSG mice was confirmed with significant differences between sham and ICR groups for villus height, crypt fission (Fig. 4b–d), crypt depth and smooth muscle layer thickness (Supplementary Fig. 7a–d), whereas there was no difference in proliferative index between sham and ICR groups (data not shown). In engrafted HIOs, ICR increased villus height, crypt fission (Fig. 4e–g and Supplementary Fig. 7e,f) and proliferative index (Fig. 4h,i) compared to sham-operated groups. These findings support the hypothesis that engrafted HIOs respond to humoral factors. In addition, this model may provide insights into the humoral adaptive response following intestinal resection. Functionally, engrafted HIOs expressed active brush border enzymes and exhibited a functional intestinal epithelial barrier, as shown by a permeability assay with FITC-dextran (Supplementary Fig. 8a,b). The engrafted HIO epithelium was also capable of peptide uptake, reflecting the existence of absorptive functions (Supplementary Fig. 8c).

To our knowledge, this is the first report of the development of a functional model for human small intestine *in vivo* derived from hPSCs. Our study highlights the potential of both ESCs and iPSCs to produce diverse cell types and tissue layers that mature following engraftment. Furthermore, the adaptive response seen in our human grafts following surgical resection in mouse hosts supports the role of humoral factors in this adaptive response and validates the use of our model for further *in vivo* studies of human small intestine. HIOs may also serve, through further translational research, as a means for the eventual treatment of short bowel syndrome and other gastrointestinal diseases, as they serve as a way to ‘personalize’ and bioengineer functional human intestine.

ONLINE METHODS

Animals

Immune-deficient NOD-SCID IL-2Rγ^{null} (NSG) mice, 8–16 weeks old, were used in all experiments (obtained from the Comprehensive Mouse and Cancer Core Facility, Cincinnati, Ohio). All mice were housed in the animal facility at the Cincinnati Children’s

Hospital Medical Center (CCHMC). All experiments were performed with the approval of the Institutional Animal Care and Use Committee of CCHMC.

Generation and maintenance of human intestinal organoids

Human intestinal organoids were generated and maintained as previously described[5,6]. Human embryonic stem cells and induced pluripotent stem cells were grown in feeder-free conditions in six-well Nunclon surface plates (Nunc) coated with Matrigel (BD Biosciences) and maintained in mTESR1 media (Stem Cell Technologies). For induction of definitive endoderm (DE), human ES or iPS cells were passaged with Dispase or Accutase (Invitrogen) and plated at a density of 100,000 cells per well in a Matrigel-coated, Nunclon surface 24-well plate. For Accutase split cells, 10 μM Y27632 compound (Sigma) was added to the media for the first day. Cells were allowed to grow until they reached 80–95% confluence. Cells were then treated with 100 ng ml^{-1} of Activin A for 3 d as previously described[27]. DE was then treated with hindgut induction medium (RPMI 1640, 2 mM L-glutamine, 2% decomplemented FBS, penicillin- streptomycin and 100 ng ml^{-1} Activin A) for 4 d with 500 ng mL^{-1} FGF4 (R&D) and 3 μM Chiron 99021 (Tocris) to induce formation of mid-hindgut spheroids. Spheroids were then plated in Matrigel (BD) and maintained in intestinal growth medium (Advanced DMEM/F-12, N2, B27, 15 mM HEPES, 2 mM L-glutamine, penicillin-streptomycin) supplemented with 100 ng ml^{-1} EGF (R&D) and 100 ng ml^{-1} Noggin (R&D) to generate human intestinal organoids (HIOs). Media was changed at 3 d with Noggin removed and then changed twice weekly thereafter. HIOs were replated in fresh Matrigel every 14 d.

Generation and characterization of induced pluripotent stem cell lines

For iPSC generation, fibroblasts were transduced with recombinant VSV-G–pseudotyped polycistronic lentiviral particles co-expressing reprogramming factors Oct4, Klf4, Sox2, cMyc and dTomato[28]. Nucleofected fibroblasts were then plated on hESC-qualified Matrigel, and 3–5 d post transduction, MEF media was replaced with mTeSR1, and cultures were subsequently fed daily with mTeSR1. After ~3 weeks, putative iPSC colonies were identified and exposed to dispase for 5 min. Discrete colonies were manually excised and replated in mTeSR1 on Matrigel-coated dishes. Several lines with typical hESC-like morphology were then expanded independently in mTeSR1 on Matrigel-coated dishes. For passaging, iPSCs were exposed to dispase for 5 min, washed, and gently triturated before replating. iPSC lines were cryopreserved in mFreSR (StemCell Technologies). All cultures were maintained in a 5% CO_2/air environment. All the experiments with iPSCs in this study were approved by institutional Embryonic Stem Cell Research Oversight (ESCRO).

For analysis of pluripotency marker expression, iPSC cultures were fixed for 10 min at room temperature with 3.7% paraformaldehyde in PBS. Cells were then permeabilized for 10 min with PBS containing 0.5% Triton X-100 and incubated for 30 min at room temperature in blocking buffer (10% normal donkey serum in PBS). Antibodies to human Oct4 (Santa Cruz, sc-5279) and Nanog (Abcam, ab21624) were diluted in blocking buffer at 1:500 and incubated with cells overnight at 4 °C. After incubation with fluorescent-labeled secondary antibodies, cultures were visualized using fluorescent microscopy. 4′,6-diamidino-2-phenylindole (DAPI) was used for nuclear counterstaining (Supplementary Fig. 9a,b).

Standard G-banded karyotype analyses of iPSCs was performed by the Cytogenetics Laboratory at Cincinnati Children's Hospital Medical Center. At least 20 metaphases were analyzed (Supplementary Fig. 9c). Analysis of *in vivo* differentiation capacity was assessed with teratoma assays. Undifferentiated iPSCs were injected subcutaneously into immune compromised NOD/SCID GAMMA $C^{-/-}$ mice. Teratomas formed within 6–12 weeks. Teratomas were excised, fixed, embedded in paraffin, sectioned and stained with H&E for histological examination (Supplementary Fig. 9d).

Generation of LGR5:eGFP BAC transgenic reporter hESC line

The LGR5: eGFP bacterial artificial chromosome (BAC) transgenic reporter hESC line was generated. In summary, the BAC RP11-59F15 was obtained from the Children's Hospital Oakland Research Institute (http://bacpac.chori.org/) and grown in SW10535 cells. A single colony was expanded in LB +cam at 32 °C, and recombineering proteins were induced by incubation at 42 °C for 20 min. The recombination cassette consisted of eGFP-FRT-PGKgb2-neo/ kan-FRT, 50-bp homology region in LGR5, and a 20-bp homology region to peGFP-PGKneo. The homology regions were selected to replace the initiator methionine of LGR5 with that of eGFP followed by a bovine growth hormone polyadenylation signal and FRT-flanked bifunctional kanamycin/G418 resistance cassette. The recombination cassette was electroporated into SW105 cells, and cells were selected on plates with cam and kanamycin (kan; 50 μg ml^{-1}). Clones were analyzed for properly targeted LGR5 BAC by PCR and confirmed by sequencing and nucleofected into single-cell suspensions of H9 hESCs using the Amaxa Human Stem Cell Nucleofector Starter Kit. Cells were selected in G418 (200 ng ml^{-1}) for 2 weeks. G418-resistant cells were maintained in antibiotic indefinitely.

Transplantation of human intestinal organoids

NSG mice were kept on antibiotic chow (275 p.p.m. Sulfamethoxazole and 1,365 p.p.m. Trimethoprim; Test Diet). Food and water was provided *ad libitum* before and after surgeries. A single HIO, matured *in vitro* for 35 d, was removed from Matrigel, washed with cold phosphate-buffered saline (DPBS; Gibco), and embedded into purified type I collagen (rat tail collagen; BD Biosciences) 12 h before surgery to allow for formation of a solidified gel plug. These plugs were then placed into standard growth media overnight in intestinal growth medium (Advanced DMEM/F-12, B27, 15 mM HEPES, 2 mM L-glutamine, penicillin-streptomycin) supplemented with 100 ng ml^{-1} EGF (R&D). HIOs were then transplanted under the kidney capsule. Briefly, the mice were anesthetized with 2% inhaled isoflurane (Butler Schein), and the left side of the mouse was then prepped in sterile fashion with isopropyl alcohol and povidine-iodine. A small left-posterior subcostal incision was made to expose the kidney. A subcapsular pocket was created and the collagen-embedded HIO was then placed into the pocket. The kidney was then returned to the peritoneal cavity and the mice were given an IP flush of Zosyn (100 mg/kg; Pfizer Inc.). The skin was closed in a double layer and the mice were given a subcutaneous injection with Buprenex (0.05 mg/kg; Midwest Veterinary Supply). At 6 weeks following engraftment, the mice were then humanely euthanized or subjected to further experimentation.

Intestinal resections in transplanted mice

Male NSG mice that have previously been transplanted with HIOs 6 weeks prior were randomized to ileocecal resection (ICR) or sham operation. Mice were placed on liquid diet (Jevity 1Cal; Abbott) 24–48 h before surgery and were changed from antibiotic chow to liquid antibiotic (200 mg Sulfamethoxazole and 40 mg Trimethoprim oral suspension 5 mL^{-1}; Hi-Tech Pharmacal) in their drinking water (0.3 mg mL^{-1} Trimethoprim) for the remainder of the experiment. Surgeries were completed under anesthesia as described above, and the abdomen of the mouse was opened anteriorly to expose the intestine. An average of 13.6 cm of distal-most small intestine was removed in addition to the cecum as previously described[26]. Mice were kept in an incubator at 30 °C for 48 h after surgery and were then euthanized on post-operative day 7.

Culture of transplant-derived enteroids

Human enteroids were generated as previously described[12,29]. Briefly, engraftments were harvested and opened and pinned with mucosa facing upwards and then rinsed in cold PBS (Gibco). The tissues were then transferred to 2 mM EDTA (EDTA; Sigma-Aldrich) in PBS and rocked for 30 min on ice. After EDTA chelation, tissues were again washed in cold PBS, and crypts were manually removed from underlying submucosa and then filtered through a 100-μm cell strainer (Fisher Scientific). Crypts were then pelleted and resuspended in Matrigel (BD Biosciences) and overlaid with intestinal growth medium (Advanced DMEM/F-12, N2, B27, 15 mM HEPES, 2 mM L-glutamine, penicillin-streptomycin) supplemented with EGF (50 ng mL^{-1}), Noggin (100 ng mL^{-1}), R-spondin 1 (1 μg mL^{-1}) (R&D Systems), 50% Wnt3a conditioned medium, 1 mM *N*-acetylcysteine, 10 nM (Leu15)-Gastrin, 10 mM Nicotidamide, 10 μM SB202190 (Sigma-Aldrich), 500 nM A-83-01 (Tocris). 2.5 μM Thiazovivin and 2.5 μM CHIR99021 (Stemgent) were added to the medium for the first 2 d. Medium was changed every 3 d. Established enteroids were passaged over time by enzymatic (TrypLE Express, Life Technologies) and mechanical dissociation through an 18-gauge needle after 7 d in culture. Dissociated enteroids were then resuspended in PBS and pelleted before resuspension in Matrigel and culture conditions as above.

Intestinal alkaline phosphatase activity

Frozen sections were washed in PBS and blocked using donkey serum. Sections were incubated with Permanent Red working solution (Permanent Red substrate + Permanent Red chromogen; Dako) for 30 min at room temperature. Sections were then washed in PBS and mounted for imaging.

In vivo FD4 permeability assay

FITC-conjugated dextran (FD4; 4,400 MW; Sigma) was dissolved in sterile water at a final concentration of 20 mg ml^{-1}. Mice with previous transplants 8 weeks prior were then anesthetized as described above, and a left, posterior subcostal incision was made to expose the left kidney and engrafted intestinal tissue. Human engraftments were then injected each with 100 μL of FD4. Whole blood was then collected using heparinized hematocrit capillary tubes at time points 30 min and 4 h post-injection, and fluorescence intensity in murine sera

was analyzed using a fluorescent plate reader. The concentration of FITC-dextran was then determined by comparison to the FITC-dextran standard curve dissolved in water.

In vivo tomato lectin injections

Fluorescein *Lycopersicon esculentum* (tomato) lectin (Vector laboratories) was resuspended in PBS at a final concentration of 2 mg ml^{-1}. 8 weeks after HIO transplantation, mice were placed under anesthesia as described above and were each injected with 200 μl of the tomato lectin via the tail vein. Mice were then humanely euthanized 30 min following injection, and tissues were collected for imaging.

In vivo D-Ala-Leu-Lys-AMCA uptake study

D-Ala-Leu-Lys-7-amido-4-methylcoumarin (D-Ala-Leu-Lys-AMCA; Sigma) was prepared as previously described[30] with modification for a final concentration of 25 μM solution in DMEM (Dulbecco's Modified Eagle Medium; Gibco). Mice were anesthetized as described above and a left posterior subcostal incision was created to expose the engraftment. The engraftment lumen was then injected with 100 μL of D-Ala-Leu-Lys-AMCA, and mice were closed in a double-layer fashion. Mice were euthanized 30 min post-injection, and tissue was collected for analysis. For comparison, engraftments were also injected with vehicle (DMEM solution) alone or with peptide solution mixed with 1 mM Captopril (Sigma), a competitive inhibitor of peptide uptake.

Tissue processing, immunofluorescence and microscopy

Tissues were fixed for 2 h to overnight in 4% paraformaldehyde (PFA). Organoid engraftments were frozen in OCT, whereas mouse intestinal tissues were embedded in paraffin. OCT sections were blocked using donkey serum (10% serum in 1× PBS plus 0.5% Triton-X) for 30 min and incubated with primary antibody overnight at 4 °C. Slides were then washed and incubated in secondary antibody in blocking buffer for 2 h at room temperature (23 °C). Paraffin sections were deparaffinized, subjected to antigen retrieval, and stained in a similar fashion to OCT sections. Please see Supplementary Table 1 for a list of antibodies and respective dilutions. Slides were then washed and mounted using ProLong Gold antifade reagent with DAPI (Life Technologies). Images were captured on a Nikon Eclipse T*i* and analyzed using Nikon Elements Imaging Software (Nikon). For transmission electron microscopy (TEM), tissues were fixed overnight in 3% glutaraldehyde in 0.175 M sodium cacodylate buffer pH 7.4. Samples were then post fixed in 1% Osmium tetroxide in 0.175 M cacodylate buffer for 1 h at 4 °C. Samples were washed and put through a series of graded ethanol (25, 50, 75, 95, 2× 100%). Infiltration was performed with 2× Propylene Oxide followed by graded infiltration with LX-112. Samples were placed in polymerization oven at 37 °C overnight and then kept at 60 °C for 3 d. A Hitachi H7600 transmission electron microscope was used to image TEM sections. For whole-mount staining, tissues were processed similarly as above and then cleared in Murray's solution. Imaging was performed with a Nikon A1 confocal microscope.

RNA isolation and RT-qPCR

RNA was extracted using RNeasy Plus Mini Kit (Qiagen) according to manufacturer's protocols. A cDNA reverse transcription kit (Applied Biosystems) was used to synthesize cDNA. Taqman (Applied Biosystems) gene expression assays were then performed on triplicate samples using a OneStep cycler (Applied Biosystems). See Supplementary Table 2 for a list of Taqman probes used.

Morphometric and statistical analyses

Histological sections were stained with hematoxylin and eosin or subjected to immunohistochemistry (as described above). All histological samples were counted in a blinded manner. Crypt depth, villus height, and smooth muscle layer (tunica muscularis) thickness were measured for a minimum of 100 well-oriented crypt-villus units or smooth muscle layer segments per mouse and then averaged using Nikon NIS imaging software. Crypt fission was also calculated in a similar manner using longitudinal sections to determine the percentage of fissioning crypts from at least 100 intact crypts per animal. A fissioning crypt is defined as a bifurcating crypt with a bisecting fissure creating two (or sometimes more) flask-shaped bases with a shared single crypt-villus junction (Supplementary Fig. 4a,f)[26]. Proliferative index was determined by injecting mice with 5-ethynyl-2′-deoxyuridine (Edu) 2 h before killing, and then, following routine Edu immunohistochemistry according to manufacturer's instructions, proliferative index was determined by calculating the ratio of Edu-positive cells to total cells within at least 10 intact crypts. All data are represented as mean ± s.e.m. *t*-tests and two-way analysis of variance were completed using Prism (GraphPad). The determined significance cutoff was $P < 0.05$. No statistical method was used to predetermine sample size.

The experiments were not randomized except ICR experiments, where transplanted animals were randomly assigned to a sham or an ICR group. The investigators were not blinded to allocation during experiments and outcome assessment except for the morphometric analysis for the ICR experiments.

Supplementary Material

Refer to Web version on PubMed Central for supplementary material.

Acknowledgments

This project was supported in part by US National Institutes of Health (NIH) grants NIH-DK092456 (J.M.W. and N.F.S.), NIH-U18NS080815 and R01DK098350 (J.M.W.), NIH-DK092306 and NIH-CA142826 (N.F.S.), NIH-R01DK083325 (M.A.H.), NIH P30 DK078392 (Digestive Health Center, Cincinnati Children Hospital Medical Center), NIH UL1RR026314 (Clinical and Translational Science Awards (CTSA), University of Cincinnati), NIH-DK36729 (G.G.), NIH-K01DK091415 (J.R.S.), NIH-P30DK034933 (University of Michigan) and NIH-DK094775 (S.R.F.).

References

1. Cheng X, et al. Self-renewing endodermal progenitor lines generated from human pluripotent stem cells. Cell Stem Cell. 2012; 10:371–384. [PubMed: 22482503]
2. Wells JM, Spence JR. How to make an intestine. Development. 2014; 141:752–760. [PubMed: 24496613]

3. Lahar N, et al. Intestinal subepithelial myofibroblasts support *in vitro* and *in vivo* growth of human small intestinal epithelium. PLoS ONE. 2011; 6:e26898. [PubMed: 22125602]
4. Levin DE, et al. Human tissue-engineered small intestine forms from postnatal progenitor cells. J Pediatr Surg. 2013; 48:129–137. [PubMed: 23331805]
5. Spence JR, et al. Directed differentiation of human pluripotent stem cells into intestinal tissue *in vitro*. Nature. 2011; 470:105–109. [PubMed: 21151107]
6. McCracken KW, Howell JC, Wells JM, Spence JR. Generating human intestinal tissue from pluripotent stem cells *in vitro*. Nat Protoc. 2011; 6:1920–1928. [PubMed: 22082986]
7. Williamson RC, Buchholtz TW, Malt RA. Humoral stimulation of cell proliferation in small bowel after transection and resection in rats. Gastroenterology. 1978; 75:249–254. [PubMed: 669211]
8. Juno RJ, et al. A serum factor after intestinal resection stimulates epidermal growth factor receptor signaling and proliferation in intestinal epithelial cells. Surgery. 2002; 132:377–383. [PubMed: 12219038]
9. Juno RJ, Knott AW, Erwin CR, Warner BW. A serum factor(s) after small bowel resection induces intestinal epithelial cell proliferation: effects of timing, site, and extent of resection. J Pediatr Surg. 2003; 38:868–874. [PubMed: 12778383]
10. Simon-Assmann P, Turck N, Sidhoum-Jenny M, Gradwohl G, Kedinger M. *In vitro* models of intestinal epithelial cell differentiation. Cell Biol Toxicol. 2007; 23:241–256. [PubMed: 17171431]
11. Jung P, et al. Isolation and *in vitro* expansion of human colonic stem cells. Nat Med. 2011; 17:1225–1227. [PubMed: 21892181]
12. Sato T, et al. Long-term expansion of epithelial organoids from human colon, adenoma, adenocarcinoma, and Barrett's epithelium. Gastroenterology. 2011; 141:1762–1772. [PubMed: 21889923]
13. Campbell FC, Tait IS, Flint N, Evans GS. Transplantation of cultured small bowel enterocytes. Gut. 1993; 34:1153–1155. [PubMed: 8406143]
14. Agopian VG, Chen DC, Avansino JR, Stelzner M. Intestinal stem cell organoid transplantation generates neomucosa in dogs. J Gastrointest Surg. 2009; 13:971–982. [PubMed: 19165549]
15. Avansino JR, Chen DC, Hoagland VD, Woolman JD, Stelzner M. Orthotopic transplantation of intestinal mucosal organoids in rodents. Surgery. 2006; 140:423–434. [PubMed: 16934605]
16. Tait IS, Evans GS, Flint N, Campbell FC. Colonic mucosal replacement by syngeneic small intestinal stem cell transplantation. Am J Surg. 1994; 167:67–72. [PubMed: 8311142]
17. Tait IS, Flint N, Campbell FC, Evans GS. Generation of neomucosa *in vivo* by transplantation of dissociated rat postnatal small intestinal epithelium. Differentiation. 1994; 56:91–100. [PubMed: 8026650]
18. Fordham RP, et al. Transplantation of expanded fetal intestinal progenitors contributes to colon regeneration after injury. Cell Stem Cell. 2013; 13:734–744. [PubMed: 24139758]
19. Yui S, et al. Functional engraftment of colon epithelium expanded *in vitro* from a single adult Lgr5(+) stem cell. Nat Med. 2012; 18:618–623. [PubMed: 22406745]
20. Kosinski C, et al. Indian hedgehog regulates intestinal stem cell fate through epithelial-mesenchymal interactions during development. Gastroenterology. 2010; 139:893–903. [PubMed: 20542037]
21. McLin VA, Henning SJ, Jamrich M. The role of the visceral mesoderm in the development of the gastrointestinal tract. Gastroenterology. 2009; 136:2074–2091. [PubMed: 19303014]
22. Zorn AM, Wells JM. Vertebrate endoderm development and organ formation. Annu Rev Cell Dev Biol. 2009; 25:221–251. [PubMed: 19575677]
23. Gracz AD, et al. Brief report: CD24 and CD44 mark human intestinal epithelial cell populations with characteristics of active and facultative stem cells. Stem Cells. 2013; 31:2024–2030. [PubMed: 23553902]
24. Kroon E, et al. Pancreatic endoderm derived from human embryonic stem cells generates glucose-responsive insulin-secreting cells *in vivo*. Nat Biotechnol. 2008; 26:443–452. [PubMed: 18288110]

25. Kovalenko PL, Basson MD. The correlation between the expression of differentiation markers in rat small intestinal mucosa and the transcript levels of schlafen 3. JAMA Surg. 2013; 148:1013–1019. [PubMed: 24005468]

26. Dekaney CM, et al. Expansion of intestinal stem cells associated with long-term adaptation following ileocecal resection in mice. Am J Physiol Gastrointest Liver Physiol. 2007; 293:G1013–G1022. [PubMed: 17855764]

27. D'Amour KA, et al. Efficient differentiation of human embryonic stem cells to definitive endoderm. Nat Biotechnol. 2005; 23:1534–1541. [PubMed: 16258519]

28. Warlich E, et al. Lentiviral vector design and imaging approaches to visualize the early stages of cellular reprogramming. Mol Ther. 2011; 19:782–789. [PubMed: 21285961]

29. Wang F, et al. Isolation and characterization of intestinal stem cells based on surface marker combinations and colony-formation assay. Gastroenterology. 2013; 145:383–395. e1–e21. [PubMed: 23644405]

30. Groneberg DA, et al. Intestinal peptide transport: *ex vivo* uptake studies and localization of peptide carrier PEPT1. Am J Physiol Gastrointest Liver Physiol. 2001; 281:G697–G704. [PubMed: 11518682]

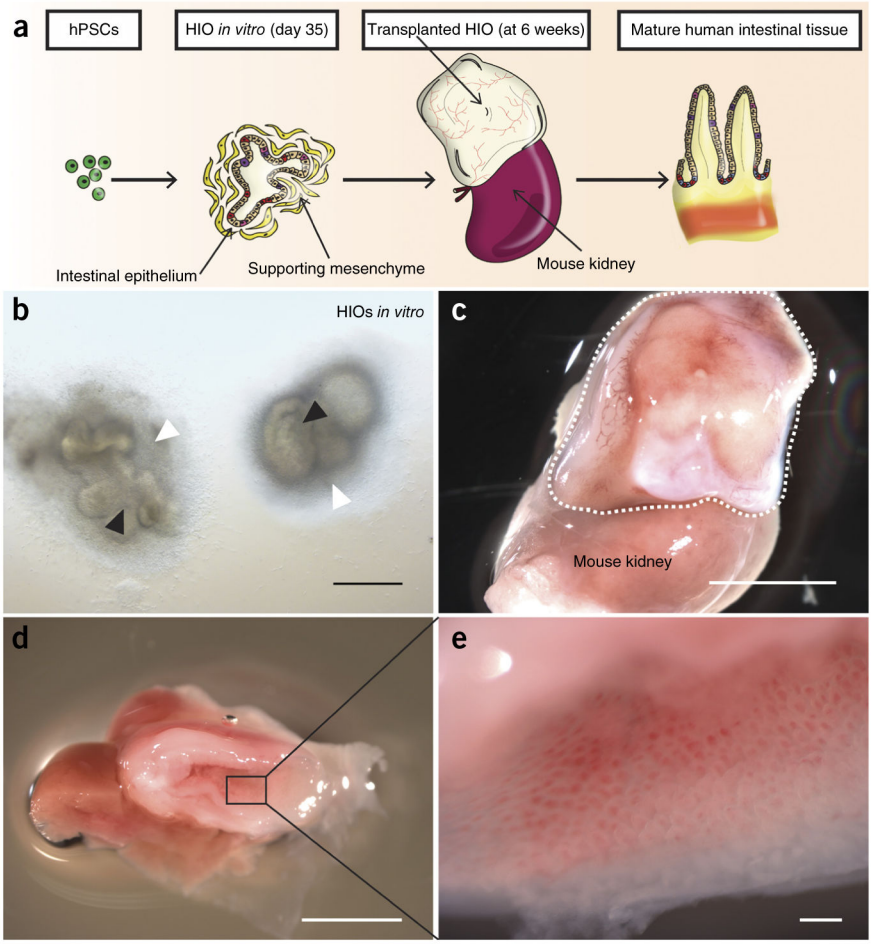

Figure 1.

HIOs engraft *in vivo* to form mature intestinal tissue. (**a**) Schematic representing development of HIOs from hPSCs and transplantation under kidney capsule to produce mature human intestinal tissue. (**b**) Two HIOs *in vitro* at 35 d consisting of intestinal epithelium (black arrowheads) surrounded by supporting mesenchyme (white arrowheads). Scale bar, 100 μm. (**c**) Engraftment (outlined) after 6 weeks with complex structure and established peripheral capillary network. The mouse kidney is seen below the engraftment for size comparison. Scale bar, 5 mm. (**d**) Cross-section of engraftment at 6 weeks revealing intestinal structure with central lumen. Scale bar, 5 mm. (**e**) Magnified luminal surface of engraftment displaying sheet of villi each with its own central capillary. Scale bar, 500 μm. *n* = 139 translplants.

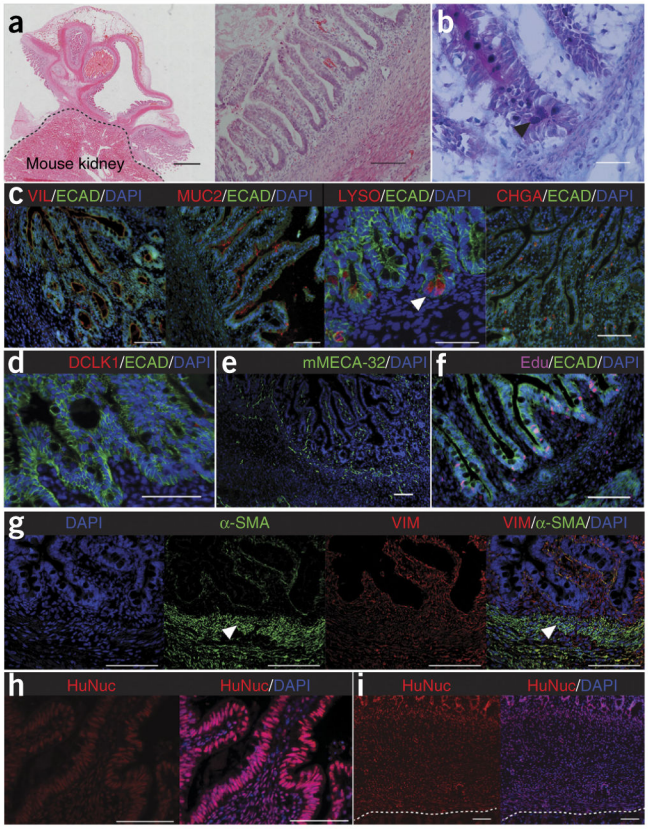

Figure 2.

Engrafted intestinal tissue resembles adult intestine and is almost entirely of human origin. (**a**) Low- and high-power imaging following H&E staining of engrafted HIO. Low magnification imaging demonstrates multiple areas of epithelium, laminated layers of smooth muscle and peripheral capillaries. Scale bars, 500 μm. High magnification imaging demonstrates crypt-villus domains as well as appropriate layers of subepithelium including lamina propria, muscularis mucosa, submucosa and outer smooth muscle layers. (**b**) Alcian blue–periodic acid–Schiff staining of epithelium within engraftment revealing secretory lineages within the crypt-villus axis. Black arrowhead points to PAS-labeled Paneth cells present within crypt bases. (**c**) All four intestinal lineages were present in engraftments including enterocytes (VIL), goblet cells (MUC2), Paneth cells (LYSO; white arrowhead; scale bars, 50 μm) and enteroendocrine cells (CHGA). E-cadherin (ECAD) was used for additional epithelial staining. (**d**) Tuft cells are also seen throughout the epithelium, as labeled with doublecortin-like kinase 1 (DCLK1). (**e**) mMECA-32 staining of mouse host vasculature ingrowth. (**f**) Edu staining of active proliferation within crypt bases and proliferative zones within crypts of epithelium. (**g**) Staining for VIM reveals the contribution of supporting mesenchyme, including laminated smooth muscle (white arrowheads) with staining of α-SMA. Merged images show dual staining with VIM and α-SMA, revealing a pericryptal sheath of supporting ISEMFs. (**h**,**i**) Contribution of human epithelial cells (**h**) and human mesenchymal tissue (**i**), as assessed by HuNuc staining through the full thickness of the engraftment. Dotted line separates engraftment from mouse kidney below. All scale bars are 100 μm except where specified otherwise. *n* = 134 transplants.

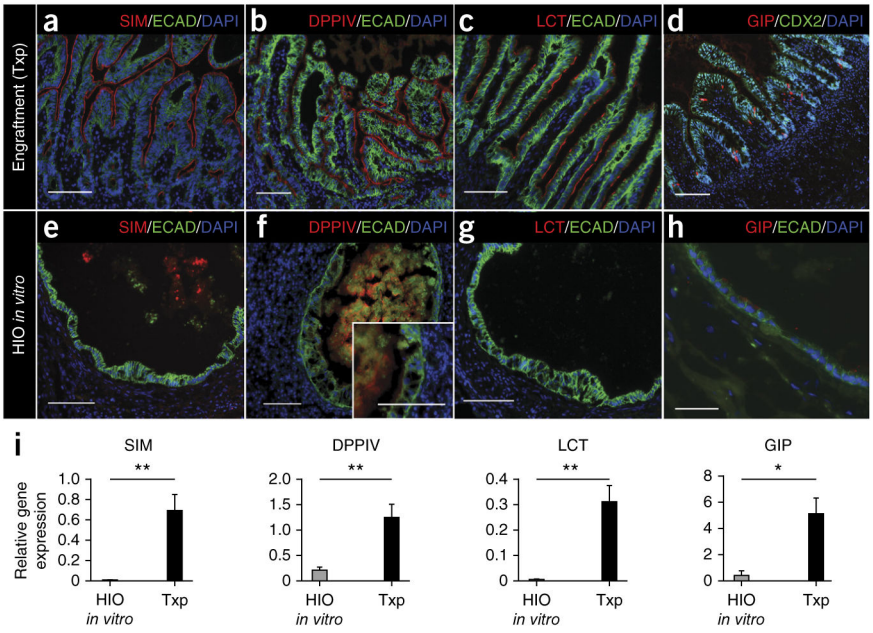

Figure 3.

Engrafted tissue matures *in vivo* and resembles mature small intestine. (**a**–**d**) Immunostaining of engrafted intestinal tissue (*in vivo*) revealing maturity of brush-border enzymes including SIM (**a**), DPPIV (**b**), LCT (**c**) and the differentiated enteroendocrine cell subtype (GIP) (**d**). ECAD and CDX2 were used for additional epithelial staining. (**e**–**h**) Staining of HIOs *in vitro* at comparable time points to transplants for SIM (**e**), DPPIV **(f)**, LCT (**g**) or GIP for comparison (**h**). (**i**) Relative gene expression of LCT, SIM, DPPIV and GIP in HIOs *in vitro* as compared to transplanted (Txp) HIOs. Values in graphs represent mean ± s.e.m.; **P* < 0.05; ***P* < 0.01; *t*-test. HIOs *in vitro:* *n* = 4; transplants (Txp): *n* = 8. Scale bars, 100 μm.

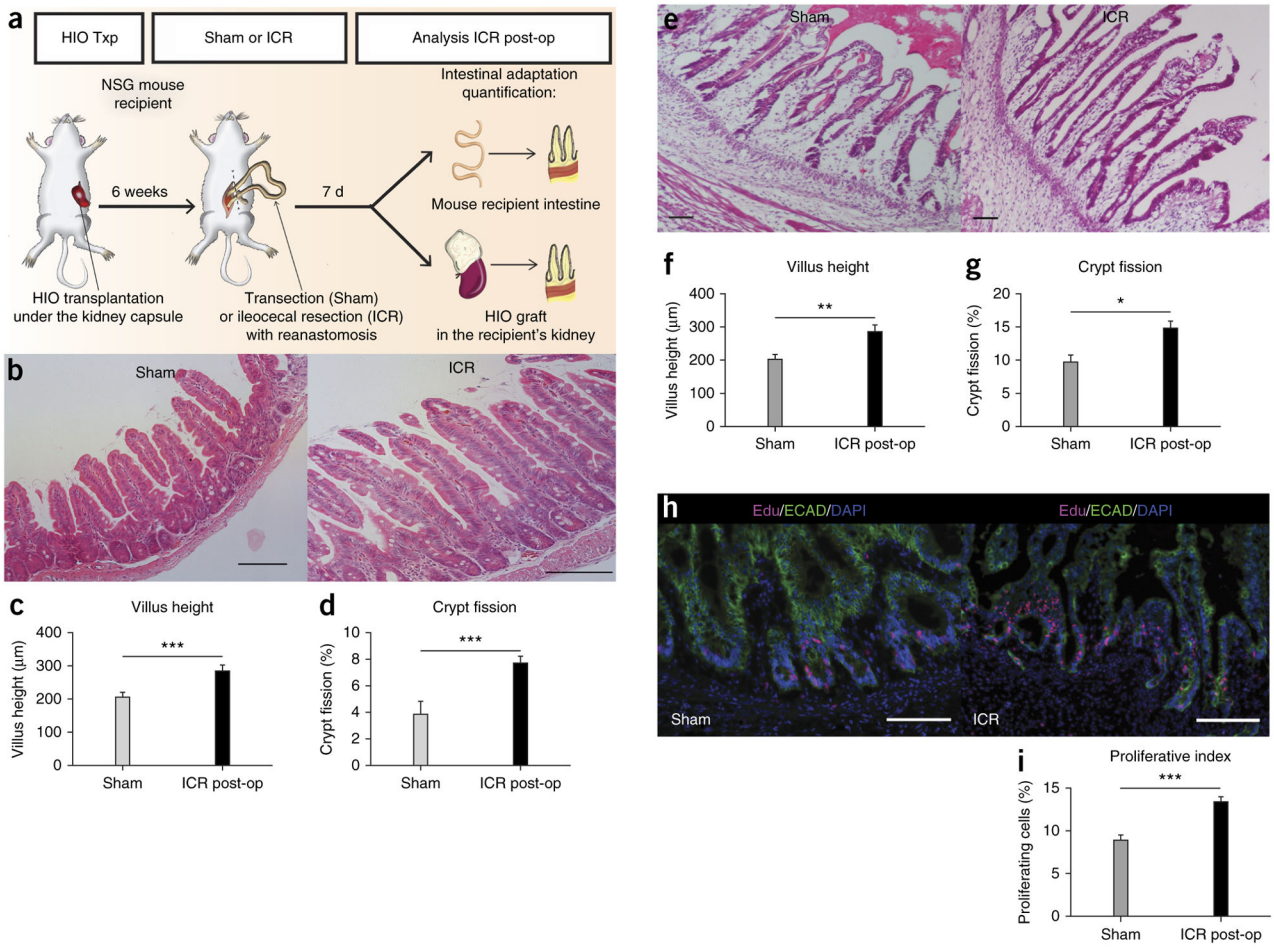

Figure 4.

Engrafted human intestinal tissue responds to humoral factors following ileocecal resection (ICR) in the mouse host. (**a**) Schematic representing resection experiments in mice with transplanted HIOs. (**b**) H&E staining of murine epithelium in sham versus ICR groups. Comparison of measured villus height (μm; **c**) and percentage of crypt fission (**d**) in mouse intestine between sham and ICR groups. (**e**) H&E staining of engrafted HIO epithelium in sham versus ICR groups. Comparison of villus height (**f**) and percentage of crypt fission (**g**) within engrafted HIOs in sham group versus ICR groups. (**h**) Immunofluorescence staining using Edu as a marker of intestinal cell proliferation in sham and ICR groups. ECAD is used to stain the epithelium. (**i**) Comparison of proliferative index (%) between sham and ICR groups in engrafted HIOs where proliferative index = number of Edu^+ cells divided by total number of cells within intestinal crypt. Scale bars, 100 μm. Values in graphs represent mean ± s.e.m. **P* < 0.05; ***P* < 0.01; ****P* < 0.001; *t*-test. Sham group: *n* = 4; ICR group: *n* = 8.